Preparation of Activated and Non-Activated Carbon from *Conocarpus* Pruning Waste as Low-Cost Adsorbent for Removal of Heavy Metal Ions from Aqueous Solution

Ahmed H. El-Naggar,[a,b] Abdalwahab K. R. Alzhrani,[c] Mahtab Ahmad,[a] Adel R. A. Usman,[a,d] Dinesh Mohan,[e] Yong Sik Ok,[f] and Mohammad I. Al-Wabel [a,*]

Conocarpus pruning waste, an agricultural byproduct, was converted into low-cost activated and non-activated carbons and used for the remediation of Cd^{2+}, Cu^{2+}, and Pb^{2+} from aqueous solutions. The carbonization was carried out at 400 °C, while the activation was carried out in the presence of KOH and $ZnCl_2$. Batch single-solute and multi-solute equilibrium and kinetic experiments were carried out to determine the adsorption capacities of the prepared activated and non-activated carbons, and these were further compared with commercially available activated carbon. The results showed that KOH-activated carbon (CK) outperformed the other activated and non-activated carbons in terms of adsorption efficiency. CK removed >50% of the applied Cd^{2+} and Cu^{2+} and 100% of Pb^{2+} at the initial concentration of 40 mg L^{-1}. Interestingly, the performance of *Conocarpus*-derived non-activated carbon was better than that of the commercial activated carbon, as observed from the Langmuir maximum adsorption capacities of 65.61, 66.12, and 223.05 µmol g^{-1} for Cd^{2+}, Cu^{2+}, and Pb^{2+}, respectively. The Pb^{2+} was the metal most easily removed from aqueous solution because of its large ionic radius. The kinetic dynamics were well described by the pseudo-second order and Elovich models.

Keywords: Chemical activation; Carbonization; Adsorption; Kinetic dynamics; Competitive effect

*Contact information: a: Soil Sciences Department, College of Food & Agricultural Sciences, King Saud University, P.O. Box 2460, Riyadh 11451, Saudi Arabia; b: Soil Sciences Department, Faculty of Agriculture, Ain Shams University, 68 Hadayek Shobra, P.O. Box 11241, Cairo, Egypt; c: Department of Botany and Microbiology, College of Science, King Saud University, P.O. Box 93702, Riyadh 11683; d: Faculty of Agriculture, Soil Science Department, Assiut University, Egypt; e: School of Environmental Sciences, Jawaharlal Nehru University, New Delhi 110067, India; f: Korea Biochar Research Center and Department of Biological Environment, Kangwon National University, Chuncheon 200-701, Republic of Korea; *Corresponding author: malwabel@ksu.edu.sa*

INTRODUCTION

Activated carbon (AC) is the most widely used adsorbent for water purification, desalination, and domestic and industrial wastewater treatment (Babel and Kurniawan 2003). To meet the increasing demands for fresh water, the water purification industry has been rapidly developing throughout the world, and there has been a remarkable increase in the AC price since the early 1990s (Marsh and Rodríguez-Reinoso 2006). It is estimated that the global demand for AC will increase by >10% *per annum* through 2016 (WAC 2012). Commercial ACs are produced using wood, coal, biomass, and agricultural and industrial wastes (Dias *et al*. 2007; Kundu *et al*. 2014). Therefore, there is a need to explore resources for the production of alternatives to the highly priced commercially available ACs. This can be achieved by utilizing locally available agricultural wastes or byproducts.

Conocarpus erectus L. is a durable evergreen tree native to North America, the coast of Central America, and tropical Africa (West 1977). Because of its rapid growth and tolerance for drought and negative environmental conditions, it is widespread in Saudi Arabia (Hegazy *et al*. 2008). Every year huge amounts of *Conocarpus* waste are either buried in landfills or burned in open fields. Converting *Conocarpus* pruning waste into AC would offer the dual benefits of reducing green waste disposal and supplying a cheap source of AC production.

Generally, carbonization and activation are the two steps involved in producing AC. Activation can be achieved by physical or chemical processes (Chen *et al*. 2012). Chemical activation is preferred, as the physical activation of carbon requires a long residence time and very high temperatures (800 to 1000 °C), while chemical activation can be achieved at lower temperatures (400 to 800 °C) (Cobb *et al*. 2012). The simultaneous carbonization and activation in a chemical activation process further reduces the AC production time. A strong acid, strong base, or salt are used for the chemical activation (Soleimani and Kaghazchi 2007). Some of the mechanisms involved in the chemical activation process include the dehydration of the lignocellulosic structure of the parent material, the combination of the chemical agent with the lignocellulosic structure, and the disintegration of the lignocellulosic structure, followed by intercalation and gasification (Marsh and Rodríguez-Reinoso 2006). The salient factors determining the quality of AC include feedstock type, carbonization temperature, duration of process, and activation process (Ng *et al*. 2003).

Industrial activities are increasing exponentially in Saudi Arabia. Despite being a water-scarce country, the demand for water in the industrial sector ranges from 190 to 1,450 million cubic meters per year (Abderrahman 2000). This exponential growth of industrial activities is reflected by the parallel increase in industrial wastewater effluents rich in organic and inorganic pollutants. Therefore, there is an urgent need to treat this industrial wastewater. The reuse of treated wastewater for irrigation purposes has recently shown its potential for managing the increasing demand for water for agriculture production in the Kingdom (Al-Jasser 2011). In this context, low-cost AC production from locally available waste resources, and its application for wastewater treatment, could be a promising solution.

In this study, *Conocarpus* pruning waste was used as a feedstock. Chemical activation was carried out using $ZnCl_2$ and KOH. The efficacy of produced ACs was determined for Cd^{2+}, Cu^{2+}, and Pb^{2+} adsorption from water. Batch equilibrium and kinetic experiments were conducted to optimize the adsorption conditions.

EXPERIMENTAL

Preparation of Activated and Non-Activated Carbon from *Conocarpus*

Conocarpus wastes were collected from the King Saud University campus, North West of Riyadh, Saudi Arabia. Woody wastes were dried under direct sunlight until they had reached a moisture content of 4.7±0.7%, and then they were cut into small pieces (2 to 3 cm). The feedstock was further dried in an oven for 24 h at 120 °C. Part of the dried feedstock was impregnated either with $ZnCl_2$ or KOH, in 1:2 and 1:5 ratios (w/w), respectively. The mixtures were then washed with distilled water and kept in an oven for 24 h at 60 °C. The impregnated feedstock was packed in a closed stainless steel container (7 x 11 x 24 cm) and pyrolyzed at 400 °C in a muffle furnace for 2.5 h at the heating rate

of 5 °C min^{-1}. The feedstock without chemical impregnation was also pyrolyzed under identical conditions. The pyrolyzed materials were left to cool down in a glass desiccator, ground according to ASTM D4607 (1999), and washed several times with distillated water until the filtrate became Cl^- free. The materials were then dried at 105 °C for 24 h and kept in airtight plastic containers at room temperature for further analysis. The obtained ACs were thereafter referred to as CZ ($ZnCl_2$-activated), CK (KOH-activated), and CH (non-activated carbon). A commercial activated carbon (CC) obtained from Sigma-Aldrich (C2889; Saudi Arabia) was also used for comparison. The CC was a multi-purpose activated carbon, made from peat and steam-activated.

Characterization of the Adsorbents

To measure the moisture contents of the produced activated carbon, 1 g of the materials was heated at 105 °C in an oven for 24 h or until the weight had stabilized. The iodine number was measured and taken as an indication of surface area in accordance with the standard procedure (ASTM D4607 (1999)). The ash content and bulk density were measured according to ASTM D2854 (2009) and ASTM D6683 (2001) standard methods, respectively. The pH of the adsorbents was measured in a 1:25 adsorbent/water ratio using a glass electrode.

The surface morphology of the developed carbons was studied using a scanning electron microscope (SEM) (EFI, S50, Inspect, The Netherlands). The samples were mounted onto double-coated adhesive carbon conductive tabs (12 mm, PELCO, UK) and placed onto the aluminum stubs. Images were captured at an acceleration voltage of 20 kV and a magnification of 2000x.

Preparation of Adsorbate

All salts ($CdCl_2$, $CuCl_2$, and $PbCl_2$) were obtained from Sigma-Aldrich, Germany. The Cd^{2+}, Cu^{2+}, and Pb^{2+} stock solutions (1000 mg L^{-1}) were prepared in de-ionized water (Max250, Millipore, France). Single-solute working solutions of 0, 5, 10, 25, and 50 mg L^{-1} concentrations of Cd^{2+}, Cu^{2+}, and Pb^{2+} were prepared from the stock solutions for the batch adsorption experiments. For each of the three elements, a multiple-solute working solution containing 50 mg L^{-1} was prepared for the competition study. All the equilibrium and kinetic studies in single and multi-component systems were carried out at the pH of 5.0. The pH of the solutions was also recorded directly after the equilibrium had been achieved.

Batch Adsorption Experiments

The batch sorption experiments were carried out in a series of stoppered 60-mL cups. For each heavy metal, the concentration range of 0 to 50 mg L^{-1} was used to obtain the adsorption isotherms. An adsorbent dose of 1.25 g L^{-1} was applied to 40 mL of the heavy metal ions solution. To reach equilibrium, the mixtures were agitated for 90 min at 25±2 °C using a mechanical orbital shaker (GFL, 3017, Germany) set at 150 rpm. The solutions were then centrifuged at 5000 rpm for 10 min to separate the adsorbents from the solution. The supernatant was then analyzed for its metal content using an inductively coupled plasma optical emission spectrometer (ICP-OES; PerkinElmer Optima 4300 DV, USA). Blanks were also run simultaneously with each batch. Three replicates of each adsorbent and blank were performed.

Adsorption Models

The adsorbed amount of each metal was calculated as a function of the metal concentration remaining in solution at equilibrium, based on Eq. 1,

$$Q_e = [(C_o - C_e)/M] \times V \quad (1)$$

where Q_e is the amount of metal adsorbed at equilibrium (mg g^{-1}); C_o and C_e are initial and equilibrium aqueous phase concentrations of the metal (mg L^{-1}); M is the weight of the adsorbent (g); and V is the volume of the metal solution (L).

The adsorption isotherms were fitted to the Langmuir and Freundlich models (Eqs. 2 and 3), respectively,

$$Q_e = q_{max}\, bC_e/(1+ bC_e) \quad (2)$$

$$x/m = K_f\, C_e\text{^}1/n \quad (3)$$

where q_{max} is the maximum adsorption capacity (mg g^{-1}) and b is the Langmuir equilibrium constant (L mg^{-1}). K_f and $1/n$ are Freundlich's adsorption capacity (mg g^{-1}) and intensity constants, respectively. Parameters of the Langmuir and Freundlich isotherms were calculated by non-linear regression using the calculation of least squares method. The curve fitting and statistical analyses were performed using SPSS software. The correlation coefficient (R^2) and standard error of the estimate (SE) obtained from regression were used for comparing the model applicability.

The statistical analyses (one way ANOVA and Tukey test) were conducted using the IBM SPSS Statistics 21 software. The data presented in the tables and figures are the averaged values of three replications, and the bars refer to standard errors.

Kinetic Experiments

The batch sorption kinetic experiments were carried out to determine the adsorption mechanism. The adsorbents (1.25 g L^{-1}) were added to each heavy metal solution (50 mg L^{-1}). The experiments were conducted in triplicate on an orbital shaker at 150 rpm. Samples were withdrawn at 0, 15, 30, 45, 60, and 90 min, centrifuged at 5000 rpm for 10 min, and the supernatants were analyzed for the final Cu^{2+}, Cd^{2+}, and Pb^{2+} concentrations using ICP-OES.

The kinetic data were simulated using different kinetic models, including the Lagergren pseudo first order model (Eq. 4), the pseudo second order model (Eq. 5), the Elovich model (Eq. 6), and the intraparticle diffusion model (Eq. 7).

$$\ln(q_e/(q_e - q_t)) = k_1\, t \quad (4)$$

$$t/q_t = 1/H_0 + 1/q_e\, t \quad (5)$$

$$H_0 = k_2\, q_e\text{^}2 \quad (5\text{-A})$$

$$q_t = \alpha \ln(a\alpha) + \alpha \ln t \quad (6)$$

$$q_t = k_{int}\, t\text{^}(1/2) \quad (7)$$

where q_e and q_t are the adsorption amounts (mg g^{-1}) at equilibrium and at time t (min), respectively; k_1 (min^{-1}) is the pseudo first order rate constant; H_0 (mg $min^{-1}g^{-1}$) is the initial adsorption rate; a is the desorption constant (g mg^{-1}); α is the Elovich initial adsorption rate (mg $g^{-1}min^{-1}$); and k_{int} is the intraparticle diffusion rate constant (mg $g^{-1}min^{-1/2}$).

RESULTS AND DISCUSSION

Characteristics of the Activated and Non-activated Carbon

The carbonization and activation processes resulted in a mass loss for the *Conocarpus* feedstock as a result of the removal of volatile materials. This was observed from the yield of ACs ranging from 67.5% to 79.2% (Table 1). The high yield of ACs could be related to the slow carbonization of the feedstock at 400 °C. The low yield of CK (67.5%) relative to CZ (78.0%) could be attributed to the high impregnation ratio of 1:5 (w/w).

The bulk density of the CK (0.49 g cm^{-3}) was greater than that of the other ACs, indicating its high filterability and adhering capacity with the adsorbate (Ekpete and Horsfall 2011).

The pH values (9.38 to 9.64) indicated that all carbons were alkaline in nature, except for the CZ (pH 6.95). The iodine number is the most important parameter in determining the AC activity. It provides a precise approximation for the surface area and microporosity of AC (Saka 2012).

Table 1. Physical and Chemical Properties of Developed Activated Carbons

Adsorbents	Yield recovery (%)	Moisture (%)	Ash content (%)	Bulk density (g cm^{-3})	pH*	Iodine Number
CC	-	3.71	1.60	0.43	9.64	800
CZ	78.0	2.76	2.00	0.43	6.95	890
CK	67.5	5.45	2.00	0.49	9.38	1126
CH	79.2	3.26	2.20	0.35	9.85	506
*1:25 adsorbent/water ratio						

A higher iodine number was observed for CK (1126) relative to CZ (890), CH (506), and CC (800), which indicated that a high degree of activation was achieved with KOH impregnation. These findings were in agreement with the previously reported studies (Sivakumar *et al*. 2012). Hydroxide activation involves H_2 generation *via* the following solid-liquid reaction, which controls the carbon activity (Lillo-Rodinas *et al*. 2004):

$$6KOH + 2C \leftrightarrow 2K + 3H_2 + 2K_2CO_3 \quad (8)$$

Likewise, chemical activation by $ZnCl_2$ also resulted in an iodine number that was about 1.8 times greater for CZ than for non-activated CH. The treatment of feedstock with $ZnCl_2$ causes "swelling" in the cellulose structure, thus breaking the cellulose molecules and creating micro- and meso-pores (Subha and Namasivayam 2009).

The surface structures of the prepared materials were investigated by SEM. The micrographs clearly indicated the differences in the porosities of the structures (Fig. 1). More micro- and meso-pores were observed in CK and CZ than were observed in the CC and CH. These findings were in line with the aforementioned iodine numbers corresponding to these ACs, thereby suggesting their greater microporosity. These diverse characteristics of the prepared ACs may have been responsible for their different adsorption capacities for the Pb^{2+}, Cu^{2+}, and Cd^{2+} in aqueous solution.

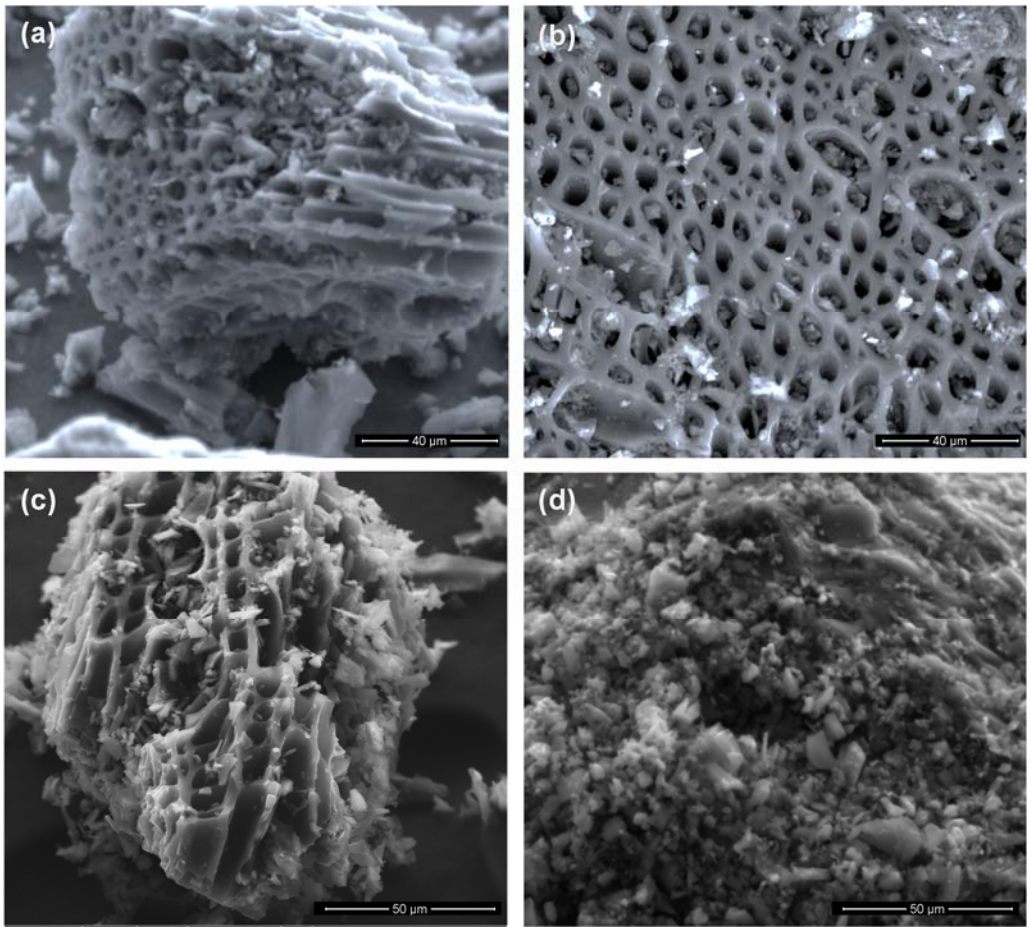

Fig. 1. SEM micrographs of (a) KOH-activated carbon (CK), (b) $ZnCl_2$-activated carbon (CZ), (c) non-activated carbon (CH), and (d) commercial activated carbon (CC)

Adsorption Kinetics

Pseudo-first order, pseudo-second order, Elovich, and intraparticle diffusion models were applied to investigate the reaction rates and adsorption mechanisms for the different ACs. The kinetic parameters calculated using the different models are presented in Table 2. The R^2 value is widely used to determine the best fit of the experimental data to the modeled data (Kumar *et al*. 2008). Based on the R^2 values obtained, the pseudo-first order equation did not describe the kinetics data (data not shown); however, all other kinetic models adequately fitted the experimental data (Table 2). The pseudo-second order model best fitted the kinetic data obtained for Cd^{2+}, Cu^{2+}, and Pb^{2+} on all ACs except for Cd^{2+} adsorption onto CZ. The adsorption capacity (q_e), the initial adsorption rate (H_0), and the rate constant (k_2) were simultaneously calculated using the model (Table 2). The q_e values followed the order CK > CH > CZ > CC for all heavy metal ions, indicating that CK was the most efficient adsorbent in removing Cd^{2+}, Cu^{2+}, and Pb^{2+} from aqueous media. The k_2 values, which determined the time required for each heavy metal to reach equilibrium, ranged from 0.02 to 0.20 g $\mu mol^{-1} min^{-1}$ for Cu^{2+}, 0.01 to 0.07 g μmol^{-1} min^{-1} for Cd^{2+}, and 0.06 to 0.16 g $\mu mol^{-1} min^{-1}$ for Pb^2. This indicated that Cd^{2+} adsorption reached equilibrium more quickly than did Cu^{2+} and Pb^{2+} adsorption. The H_0 values were higher for the adsorption of Cd^{2+} onto CK (11.32 µmol min^{-1} g^{-1}) and Pb^{2+} onto CK (99.61 µmol min^{-1} g^{-1}) than for any others showing a high initial adsorption rate.

Table 2. Kinetic Parameters of Selected Adsorption Reaction and Diffusion Models Calculated from Simulated Data of Cu^{2+}, Cd^{2+}, and Pb^{2+} Sorption onto Various Carbonaceous Materials

Adsor-bate	Adsor-bent	Kinetic models								
		Pseudo-second order				Elovich			Intraparticle diffusion	
		q_e (μmol g^{-1})	H_0 (μmol min^{-1} g^{-1})	k_2 (g μmol^{-1} min^{-1})	R^2	α (μmol g^{-1} min^{-1})	a (g μmol^{-1})	R^2	k_{int} (μmol g^{-1} $min^{-1/2}$)	R^2
Cu^{2+}	CC	1.56	0.32	0.13	0.98	0.78	3.24	0.99	0.15	0.88
	CZ	1.86	0.70	0.20	0.97	0.46	2.32	0.98	0.31	0.98
	CK	16.5	0.27	0.02	0.98	0.54	4.61	0.99	1.02	0.91
	CH	3.76	1.67	0.12	1.00	1.05	1.11	1.00	0.27	0.99
Cd^{2+}	CC	1.07	0.07	0.07	0.87	0.05	2.14	0.99	0.15	0.98
	CZ	1.73	0.03	0.01	0.32	0.05	0.99	0.97	0.19	0.97
	CK	21.0	11.32	0.03	1.00	45.3	0.47	0.98	1.26	0.96
	CH	7.09	0.68	0.01	0.91	0.42	0.40	0.87	0.75	0.95
Pb^{2+}	CC	21.7	6.35	0.08	1.00	1.75	0.45	0.99	1.50	0.95
	CZ	24.2	33.86	0.06	1.00	2.54	0.32	0.98	2.44	0.88
	CK	39.5	99.61	0.06	1.00	50.4	0.98	0.96	4.39	0.95
	CH	39.0	7.26	0.16	1.00	49.5	1.45	0.93	3.83	0.93

The kinetics adsorption data were also well described by the Elovich model (R^2 = 0.87 to 1.00) for all heavy metal ions (Table 2). The Elovich model is widely used to elaborate the adsorption of contaminants based on the heterogeneous surfaces of the sorbents (Plazinski *et al*. 2009). The initial adsorption rates (α) were in the order CK > CH > CZ > CC for both Cd^{2+} and Pb^{2+}, and in the order CH > CC > CK > CZ for Cu^{2+}, indicating high Cd^{2+} and Pb^{2+} adsorption onto CK and high Cu^{2+} adsorption onto CH.

Because of the porous structure of the adsorbents, intraparticle diffusion through micro-, meso-, and macro-pores could be another possible mechanism of Cu^{2+}, Cd^{2+}, and Pb^{2+} sorption. Therefore, the experimental adsorption data were subjected to an intraparticle diffusion model that provided a good fit of the data as indicated by the R^2 values ranging from 0.88 to 0.99 (Table 2, Fig. 2). The intraparticle diffusion rate constant (k_{int}) was higher for CK (1.02 μmol g^{-1} $min^{-1/2}$ for Cu^{2+}, 1.26 μmol g^{-1} $min^{-1/2}$ for Cd^{2+}, and 4.39 μmol g^{-1} $min^{-1/2}$ for Pb^{2+}) than for all other adsorbents, suggesting a high metal adsorption rate. The intraparticle diffusion has previously been reported by El-Ashtoukhy *et al*. (2008) as the rate-limiting step in the batch experiments of Pb^{2+} and Cu^{2+} adsorption from aqueous solution using pomegranate peel.

The adsorption dynamics revealed that CK was the most favorable choice for Cd^{2+}, Cu^{2+}, and Pb^{2+} adsorption. This could be attributed to the high activity of CK as indicated by its high iodine number value relative to other carbons. The best fit of the experimental data to the pseudo-second order and Elovich model predicted that chemisorption may be the dominating mechanism responsible for Cd^{2+}, Cu^{2+}, and Pb^{2+} adsorption onto different carbons. A model of chemisorption assumes that the adsorption is a multilayer occurrence in which each layer exhibits different activation energies (Alberti *et al*. 2012). Furthermore, the diffusion of heavy metal ions into the pores of the tested adsorbents could be another

plausible mechanism of Cd^{2+}, Cu^{2+}, and Pb^{2+} adsorption, as indicated by the good fitness of the experimental data to the intraparticle diffusion model. Specifically, the high adsorption rates for CK and CH could be due to their micro-porous structures, as can be observed from the SEM micrographs (Fig. 1).

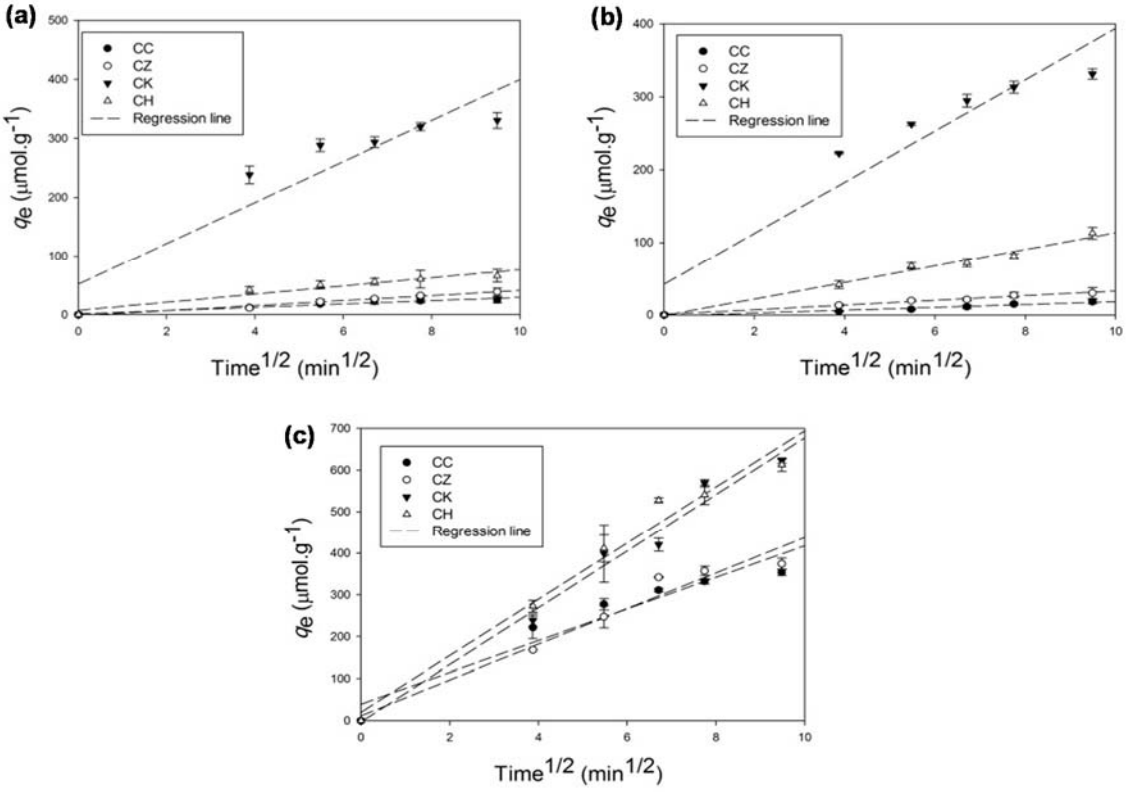

Fig. 2. Linear regression fittings of the intraparticle diffusion model for (a) Cu^{2+}, (b) Cd^{2+}, and (c) Pb^{2+} adsorption kinetics onto different adsorbents (CC, commercial activated carbon; CZ, $ZnCl_2$-activated carbon; CK, KOH-activated carbon; CH: non-activated carbon)

Adsorption Equilibrium

The Langmuir and Freundlich isotherm models were used to investigate the equilibrium relationships between the metals adsorbed onto different carbons and the metal equilibrium concentrations in solution at constant temperature. Non-linearized isotherm models were employed to avoid the error variance violation caused by linearized forms (Ho *et al*. 2002). The adsorption isotherm constants are presented in Table 3. The Langmuir adsorption isotherms obtained for the various sorbents are shown in Fig. 3. The Langmuir adsorption capacities (q_{max}) for Cd^{2+} and Cu^{2+} followed the order CK > CH > CC > CZ, while for Pb^{2+}, the adsorption capacities follow the order CH > CK > CZ > CC. The high adsorption capacities of CK and CH were also evidenced from their high binding energies (*b* values; Table 3). The extremely high q_{max} values that were obtained for CK (191.3 μmol g^{-1} for Cd^{2+}, 213.1 μmol g^{-1} for Pb^{2+}, and 399.17 μmol g^{-1} for Cu^{2+}) indicated a high adsorption capacity of CK due to its high iodine number (1126; Table 1), and also suggested that it had a high surface area relative to other carbons. The 1/*n* values of the Freundlich model were less than 1 for all sorbents, indicating a downward-curved isotherm in which the sorption of metals decreased with increases in the surface loading of the adsorbent (Site 2001).

Overall, the adsorption data were better described by the Langmuir isotherm equation (R^2 = 0.84 to 0.99) than the Freundlich isotherm equation (R^2 = 0.76 to 0.98), indicating the monolayer adsorption of the heavy metal ions onto the carbon surfaces. The high adsorption capacity of CK as predicted by the Langmuir model was in agreement with the predictions of the pseudo-second order model for the kinetics adsorption data (Table 2). Among the different heavy metal ions, Pb^{2+} showed the highest adsorption affinity onto the different carbons, which could be due to its larger ionic radius (0.118) relative to Cd^{2+} (0.097) and Cu^{2+} (0.073) (Ahmad *et al*. 2012).

Table 3. Langmuir and Freundlich Adsorption Isotherm Parameters for Cu^{2+}, Cd^{2+}, and Pb^{2+} Adsorption onto Different Carbonaceous Materials

Adsor-bents	Langmuir			Freundlich			Langmuir			Freundlich			Langmuir			Freundlich		
	Cd^{2+}						Pb^{2+}						Cu^{2+}					
	q_{max} (μmol g^{-1})	*b*	R^2	K_f	1/*n*	R^2	q_{max} (μmol g^{-1})	*b*	R^2	K_f	1/*n*	R^2	q_{max} (μmol g^{-1})	*b*	R^2	K_f	1/*n*	R^2
CC	18.64	0.01	0.84	2.59	0.20	0.89	111.73	0.10	0.98	2.80	0.11	0.88	31.27	0.00	0.97	2.04	0.48	0.87
CZ	12.49	0.17	1.00	12.95	0.02	0.80	132.58	0.08	0.98	2.08	0.17	0.87	29.69	0.02	1.00	4.88	0.08	0.76
CK	191.30	0.23	1.00	3.48	0.07	0.87	213.10	0.32	0.93	2.25	0.13	0.97	399.17	0.01	0.90	3.02	0.11	0.97
CH	65.61	0.19	0.98	4.37	0.06	0.83	223.05	0.15	0.93	1.83	0.19	0.95	66.12	0.01	0.97	5.00	0.07	0.90

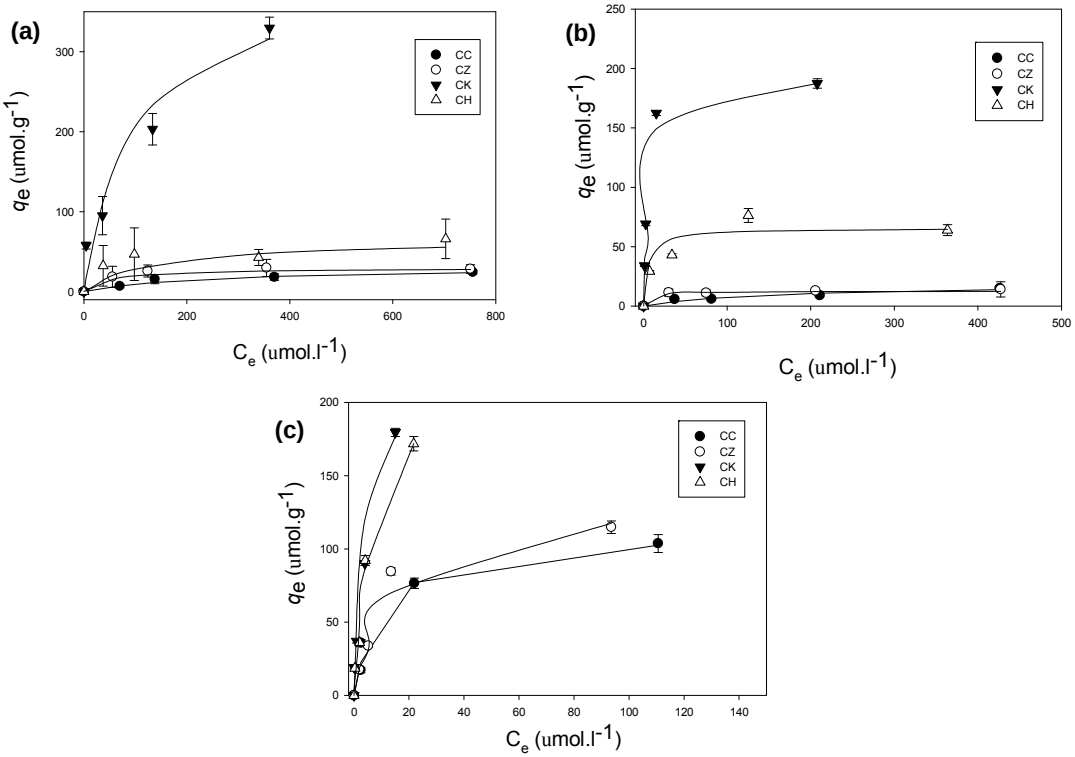

Fig. 3. The Langmuir isotherms fitted to the experimental equilibrium data of (a) Cu^{2+}, (b) Cd^{2+}, and (c) Pb^{2+} adsorption onto different adsorbents. (CC, commercial activated carbon; CZ, $ZnCl_2$ activated carbon; CK, KOH activated carbon; CH, non-activated carbon)

The non-activated CH had a higher adsorption capacity than CZ and CC for Cd^{2+}, Cu^{2+}, and Pb^{2+}. The incomplete carbonization at low temperature (400 °C) without

chemical impregnation may have resulted in the persistence of non-carbonized materials in the CH, where partitioning could be the main adsorption mechanism (Chen *et al*. 2008). Another implication is that CH contains different functional groups, including carbonyl (C=O), carboxyl (-COOH), and hydroxyl (-OH) (Al-Wabel *et al*. 2013) that may contribute to metal complexation (Ahmad *et al*. 2014). Therefore, it may be speculated that the high adsorption capacity of non-activated CH may be due to various mechanisms, including adsorption, partitioning, complexation, and pore diffusion.

Comparison with Other Studies

Sorption capacity of CK was compared with other studies using different precursors and similar activation process (*i.e.* impregnation with KOH) (Table 4). For all heavy metal ions (Cd^{2+}, Cu^{2+}, and Pb^{2+}), the sorption capacity of CK was better or comparable with other reported literature. Therefore, activated carbon produced from the *Conocarpus* pruning waste could be a cost effective alternative sorbent for the removal of heavy metal ions from aqueous media.

Table 4. Comparison of CK with other types of KOH Activated Carbons

Metal	Adsorbent	Adsorption capacity (q_{max}, mg g^{-1})	Reference
Cd^{2+}	Conocarpus pruning waste	21.50	This study
	Oil palm fiber	6.84	Aimi *et al*. 2014
	Rice husk	8.24	Haris *et al*. 2011
	Cashew nut shells	14.29	Tangjunak *et al*. 2009
	Cassava stem biochar	24.88	Prapagdee *et al*. 2014
Cu^{2+}	Conocarpus pruning waste	25.36	This study
	Olive stone waste	17.83	Alslaibi *et al*. 2014
	Coffee ground waste	21.2	Yeung *et al*. 2014
	Pine cone	26.32	Ofomaja *et al*. 2010
	Kenaf core biomass	27.78	Chowdhury *et al*. 2012a
Pb^{2+}	Conocarpus pruning waste	44.15	This study
	Mangostene fruit shells	25.00	Chowdhury *et al*. 2012b
	Cashew nut shells	28.90	Tangjunak *et al*. 2009
	Sludge	46.90	Zaini *et al*. 2014

Removal of Heavy Metal ions

The percentage removed of Cd^{2+}, Cu^{2+}, and Pb^{2+} from water by various ACs is shown in Fig. 4. At low initial metal concentrations, the removal was high, but then gradually decreased with increasing metal concentrations. The CK was most efficient in removing Cu^{2+} and Cd^{2+}, while CK and CH removed equal percentages of Pb^{2+} from aqueous solutions at all the initial concentrations. The CK was capable of removing >85% and >50% of Cd^{2+}, Cu^{2+}, and Pb^{2+} contents at the initial concentrations of 4 mg L^{-1} and 40 mg L^{-1}, respectively. The decrease in removal efficiency was due to the insufficient availability of binding sites at higher metal concentrations. Generally, it is believed that the adsorption of heavy metal ions on carbons is site-specific (Usman 2008). With the surface loading of metals increasing, fewer sites were available to adsorb more quantities of metal in the solution.

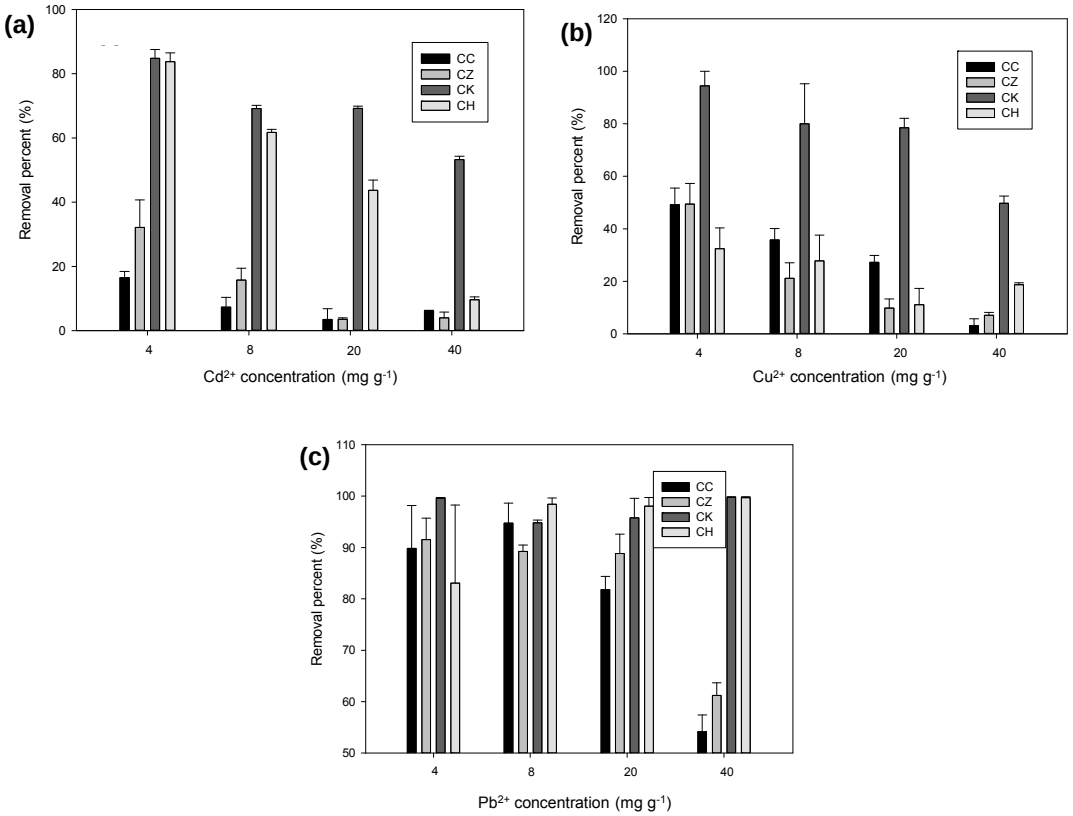

Fig. 4. The percentage removal of (a) Cd^{2+}, (b) Cu^{2+}, and (c) Pb^{2+} from aqueous solution by various adsorbents as affected by metal concentration (CC, commercial activated carbon; CZ, $ZnCl_2$ activated carbon; CK, KOH activated carbon; CH, non-activated carbon)

Competitive Adsorption

To account for the more realistic contamination of water with multiple elements, the competitive effects of Cd^{2+}, Cu^{2+}, and Pb^{2+} on their adsorption onto different adsorbents were investigated, and the results are presented in Fig. 5. In a single-solute adsorption experiment at an initial metal concentration of 50 mg L^{-1}, maximum adsorption was obtained for Pb^{2+}, followed by Cu^{2+} and/or Cd^{2+} except onto CK. Greater sorption of Cu^{2+} onto CK could be attributed to high affinity of Cu^{2+} to form $Cu(OH)_2$ than Pb^{2+} and Cd^{2+} as determined from their solubility products (K_{sp} $Cu(OH)_2$ = 1 x 10^{-20}, K_{sp} $Pb(OH)_2$ = 2.5 x 10^{-16}, and K_{sp} $Cd(OH)_2$ = 3.2 x 10^{-14}) (Gonzalez *et al*. 2015). However, in a multi-solute adsorption experiment at the same initial metal concentration, a reduction in the adsorbed amount of each heavy metal was recorded, thereby indicating a possible competition among Cd^{2+}, Cu^{2+}, and Pb^{2+} for the available adsorption sites. Additionally, Cu^{2+} showed maximum adsorption onto all adsorbents in the mixed metals solution, which contradicted its behavior in the single metal solutions, where Pb^{2+} was generally the dominantly adsorbed metal ion onto CC, CZ and CH. The dynamics of the competition between different metals for the available adsorption sites were driven by metal properties such as ionic radius, atomic weight, hydrolysis constant, electronegativity and Misono softness values (Ahmad *et al*. 2012). Moreover, the heterogeneity, pore size distribution, and hydrophobicity of the carbons also had vital impacts on the contaminant sorption in a multi-solute system (Li *et al*. 2002; Pagnanelli *et al*. 2005).

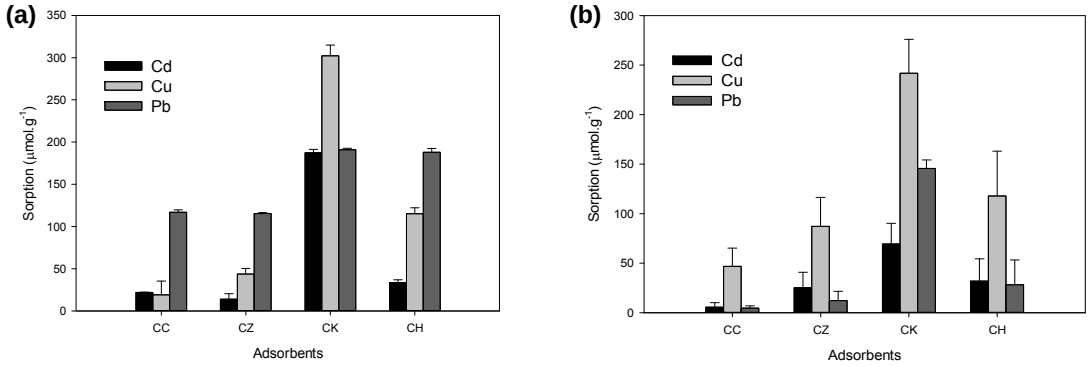

Fig. 5. (a) Single-solute and (b) multi-solute adsorption of Cd^{2+}, Cu^{2+}, and Pb^{2+} onto different adsorbents. (CC, commercial activated carbon; CZ, $ZnCl_2$-activated carbon; CK, KOH-activated carbon; CH, non-activated carbon)

Table 5. Metals Ordered According to Ionic Properties and Adsorption Values Ordered According to Adsorbents

Metal characteristics	Metal order according to its property
Atomic weight	Pb^{2+} (207.2) > Cd^{2+} (112.41) > Cu^{2+} (63.54)
Ionic radius	Pb^{2+} (1.21) > Cd^{2+} (0.97) > Cu^{2+} (0.70) Å
pK_1	Pb^{2+} (7.8) ≥ Cu^{2+} (8.0) > Cd^{2+} (10.1)
Softness	Pb^{2+} (3.58) > Cd^{2+} (3.04) > Cu^{2+} (0.70)
Electronegativity	Cu^{2+} (1.9) > Pb^{2+} (1.8) > Cd^{2+} (1.7)
Hydroxide solubility product	Cu^{2+} (1×10^{-20}) > Pb^{2+} (2.5×10^{-16}) > Cd^{2+} (3.2×10^{-14})
Adsorbents	**Selectivity sequence**
CC	$Cu^{2+} > Cd^{2+} \geq Pb^{2+}$
CZ	$Cu^{2+} > Cd^{2+} > Pb^{2+}$
CK	$Cu^{2+} > Pb^{2+} > Cd^{2+}$
CH	$Cu^{2+} > Cd^{2+} \geq Pb^{2+}$

The relative sorption selectivities of Pb^{2+}, Cu^{2+}, and Cd^{2+} by the investigated sorbents were determined, and the results are depicted in Table 5. The three investigated metals were arranged according to their adsorption capacity (μmol g^{-1}) in the following relative sequences: $Cu^{2+} > Cd^{2+} \geq Pb^{2+}$ for CC; $Cu^{2+} > Cd^{2+} > Pb^{2+}$ for CZ; $Cu^{2+} > Pb^{2+} > Cd^{2+}$ for CK; $Cu^{2+} > Cd^{2+} \geq Pb^{2+}$ for CH. The predicted order of heavy metal ions based on their properties is also shown in Table 5. It was observed that the variations in the order of the sorption capacities were dependent on the properties of both metal and the adsorbents. The order for the adsorption of heavy metal ions onto CK was correlated with the relative electronegativity of the metals and metals hydroxide ($M(OH)_2$) solubility product constants. Moreover, the adsorption preferences presented by CC, CK and CH for Cu^{2+} over the other two metals may be explained by its high electronegativity and lower ionic radius. The metal affinity order of the CK could be expected based on the fact that the metal retention is dependent on MOH^+ adsorption, and is more strongly adsorbed than the free metal. Additionally, the heavy metal ions can also be precipitated as $M(OH)_2$. Therefore, the hydrolyzed metal forms may have been the main factor affecting metal adsorption and/or precipitation onto CK. Generally, the results suggested that the adsorption preferences exhibited by CK for Pb^{2+} over the other two heavy metal ions may be explained by this heavy metal's relatively high pK1, atomic weight, and softness.

CONCLUSIONS

1. *Conocarpus* pruning waste was converted to activated and non-activated carbon. These carbons were characterized and utilized as adsorbents for aqueous Cd^{2+}, Cu^{2+}, and Pb^{2+}.
2. The Langmuir model predicted the highest adsorption capacity of the *Conocarpus*-derived KOH-activated carbon for the removal of heavy metal ions. The adsorption dynamics were adequately described by the pseudo-second order, Elovich, and intraparticle diffusion models.
3. The competition for active sites available on carbon was observed in the multi-solute system. Interestingly, the non-activated carbon derived from *Conocarpus* waste performed better than the commercially available activated carbon.
4. It is therefore recommended that *Conocarpus* waste be successfully converted into an efficient and low-cost carbon for the purification of metal-contaminated water.

ACKNOWLEDGMENTS

The authors extend their appreciation to the Deanship of Scientific Research, King Saud University for funding this work through the international research group project IRG-14-14.

REFERENCES CITED

Abderrahman, W. A. (2000). "Urban water management in developing arid countries," *Water Res. Develop.* 17, 247-255.

Ahmad, M., Usman, A. R. A., Lee, S. S., Kim, S. C., Joo, J. H., Yang, J. E., and Ok, Y. S. (2012). "Eggshell and coral wastes as low cost sorbents for the removal of Pb^{2+}, Cd^{2+} and Cu^{2+} from aqueous solutions," *J. Ind. Eng. Chem*. 18(1), 198-204. DOI: 10.1016/j.jiec.2011.11.013

Ahmad, M., Rajapaksha, A. U., Lim, J. E., Zhang, M., Bolan, N., Mohan, D., Vithanage, M., Lee, S. S., and Ok, Y. S. (2014). "Biochar as a sorbent for contaminant management in soil and water: A review," *Chemosphere* 99, 19-33. DOI: 10.1016/j.chemosphere.2013.10.071

Aimi, A. W. N., Norain, I., Aziyah, N. B., Izza, N. H., Vicinisvarri, I., and Hakim, M. H. (2014). "Utilization of base modified oil palm fiber for removal of Cd(II) from aqueous solution," *Res. J. Chem. Environ*. 18(5), 26-32.

Alberti, G., Amendola, V., Pesavento, M., and Beisuz, R. (2012). "Beyond the synthesis of novel solid phases: Review on modeling of sorption phenomena," *Coordin. Chem. Rev*. 256(1-2), 28-45. DOI: 10.1016/j.ccr.2011.08.022

Alslaibi, T. M., Abustan, I., Ahmad, M. A., and Foul, A. A. (2014). "Preparation of activated carbon from olive stone waste: Optimization study on the removal of Cu^{2+}, Cd^{2+}, Ni^{2+}, Pb^{2+}, Fe^{2+}, and Zn^{2+} from aqueous solution using response surface methodology," J. Disper. Sci. Technol. 35, 913-925. DOI: 10.1080/01932691.2013.809506

Al-Jasser, A. O. (2011). "Saudi wastewater reuse standards for agricultural irrigations: Riyadh treatment plants effluent compliance," *J. King Saud U*. 23(1), 1-8. DOI: 10.1016/j.jksues.2009.06.001

Al-Wabel, M. I., Al-Omran, A., El-Naggar, A. H, Nadeem, M., and Usman, A. R. A. (2013). "Pyrolysis temperature induced changes in characteristics and chemical composition of biochar produced from *Conocarpus* wastes," *Biores. Technol*. 130, 374-379. DOI: 10.1016/j.biortech.2012.12.165

ASTM D2854 (2009). "Standard test method for apparent density of activated carbon," ASTM International, West Conshohocken, PA. DOI: 10.1520/D2854-09

ASTM D2866 (2011). "Standard test method for total ash content of activated carbon," ASTM International, West Conshohocken, PA. DOI: 10.1520/D2866-11

ASTM D4607 (1999). "Standard test method for determination of iodine number of activated carbon," ASTM International, West Conshohocken, PA. DOI: 10.1520/D4607-94R99

ASTM D6683 (2001) "Standard test method for measuring bulk density values of powders and other bulk solids," ASTM International, West Conshohocken, PA. DOI: 10.1520/D6683-01

Babel, S., and Kurniawan, T. A. (2003). "Low-cost adsorbents for heavy metals uptake from contaminated water: A review," *J. Hazard. Mater*. 97(1-3), 219-243. DOI: 10.1016/S0304-3894(02)00263-7

Chen, B., Zhou, D., and Zhu, L. (2008). "Transitional adsorption and partition on nonpolar and polar aromatic contaminants by biochars of pine needles with different pyrolytic temperatures," *Environ. Sci. Technol*. 42(14), 5137-5143. DOI: 10.1021/es8002684

Chen, C. X., Huang, B., Li, T., and Wu, G. F. (2012). "Preparation of phosphoric acid activated carbon from sugarcane bagasse by mechanochemical processing," *BioResources* 7(4), 5109-5116. DOI: 10.15376/biores.7.4.5109-5116

Chowdhury, Z. Z., Zain, S. M., Khan, R. A., and Islam, M. S. (2012a). "Preparation and characterization of activated carbon from kenaf fiber for equilibrium sorption studies of copper from wastewater," *Korean J. Chem. Eng*. 29(9), 1187-1195. DOI: 10.1007/s11814-011-0297-9

Chowdhury, Z. Z., Zain, S. M., Khan, R. A., Rafique, R. F., and Khalid, K. (2012b). "Batch and fixed bed adsorption studies of lead(II) cations from aqueous solutions onto granular activated carbon derived from *Mangostana garcinia* shell," *BioResources* 7(3), 2895-2915. DOI: 10.15376/biores.7.3.2895-2915

Cobb, A., Warms, M., Maurer, E. P., and Chiesa, S. (2012). "Low-tech coconut shell activated charcoal production," *Int. J. Serv. Learn. Eng*. 7(1), 93-104.

Dias, J. M., Alvim-Ferraz, M. C. M., Almeida, M. F., Rivera-Utrilla, J., and Sanchez-Polo, M. (2007). "Waste materials for activated carbon preparation and its use in aqueous-phase treatment: A review," *J. Environ. Manag*. 85(4), 833-846. DOI: 10.1016/j.jenvman.2007.07.031

Ekpete, O. A., and Horsfall, M. (2011). "Preparation and characterization of activated carbon derived from fluted pumpkin stem waste (*Telfairia occidentalis* Hook F)," *Res. J. Chem. Sci*. 1(3), 10-17

El-Ashtoukhy, E. S. Z., Amin, N. K., and Abdelwahab, O. (2008). "Removal of lead(II) and copper(II) from aqueous solution using pomegranate peel as a new adsorbent," *Desalination* 223(1-3),162-173. DOI: 10.1016/j.desal.2007.01.206

Gonzalez, M. A., Pavlovic, I., and Barriga, C. (2015). "Cu(II), Pb(II) and Cd(II) sorption on different layered double hydroxides. A kinetic and thermodynamic study and competing factors", *Chem. Eng. J*. 269, 221-228. doi:10.1016/j.cej.2015.01.094

Haris, M. R. H. M., Wahab, N. A. A., Reng, C. W., Azahari, B., and Sathasivam, K. (2011). "The sorption of Cd(II) ions on mercerized rice husk and activated carbon," *Turk. J. Chem*. 35, 939-950.

Hegazy, S. S., Aref, I. M., Al-Meffarrej, H., and El-Juhany, L. I. (2008). "Effect of spacing on the biomass production and allocation in *Conocarpus erectus* L. trees grown in Riyadh, Saudi Arabia," *Saudi J. Biol. Sci*. 15(2), 315-322

Ho, Y. S., Porter, J. F., and McKay, G. (2002). "Equilibrium isotherm studies for the sorption of divalent metal ions onto peat: Copper, nickel, and lead single component systems," *Water Air Soil Poll*. 141(1-4), 1-33. DOI: 10.1023/A:1021304828010

Kumar, K. V., Porkodi, K., and Rocha, F. (2008). "Comparison of various error functions in predicting the optimum isotherm by linear and non-linear regression analysis for the sorption of basic red 9 by activated carbon," *J. Hazard. Mater*. 150(1), 158-165. DOI: 10.1016/j.jhazmat.2007.09.020

Kundu, A., Redzwan, G., Sahu, J. N., Mukherjee, S., Gupta, B. S., and Hashim, M. A. (2014). "Hexavalent chromium adsorption by a novel activated carbon prepared by microwave activation," *BioResources* 9(1), 1498-1518. DOI: 10.15376/biores.9.1.1498-1518

Li, L., Quinlivan, P. A., and Knappe, D. R. U. (2002). "Effects of activated carbon surface chemistry and pore structure on the adsorption of organic contaminants from aqueous solution," *Carbon* 40(12), 2085-2100. DOI: 10.1016/S0008-6223(02)00069-6

Lillo-Rodinas, M. A., Juan-Juan, J., Cazorla-Amoros, D., and Linares-Solano, A. (2004). "About reactions occurring during chemical activation with hydroxides," *Carbon* 42, 1371-1375. DOI: 10.1016/j.carbon.2004.01.008

Marsh, H., and Rodríguez-Reinoso, F. (2006). *Activated Carbon*, Elsevier Science, Oxford.

Ng, C., Marshall, W., Rao, R. M., Bansode, R. R., and Losso, J. N. (2003). "Activated carbon from pecan shell: Process description and economic analysis," *Ind. Crop. Prod*. 17(3), 209-217. DOI: 10.1016/S0926-6690(03)00002-5

Ofomaja, A. E., Naidoo, E. B., and Modise, S. J. (2010). "Biosorption of copper(II) and lead(II) onto potassium hydroxide treated pine cone powder," *J. Environ. Manage*. 91(8), 1674-1685. DOI: 10.1016/j.jenvman.2010.03.005

Pagnanelli, F., Mainelli, S., De Angelis, S., and Toro, L. (2005). "Biosorption of protons and heavy metals onto olive pomace: Modelling of competition effects," *Water Res*. 39(8), 1639-1651. DOI: 10.1016/j.watres.2005.01.019

Plazinski, W., Rudzinski, W., and Plazinska, A. (2009). "Theoretical models of sorption kinetics including a surface reaction mechanism: A review," *Adv. Colloid Interf. Sci*. 152(1-2), 2-13. DOI: 10.1016/j.cis.2009.07.009

Prapagdee, S., Piyatiratitivorakul, S., and Petsom, A. (2014). "Activation of cassava stem biochar by physico-chemical method for stimulating cadmium removal efficiency from aqueous solution," *Environ. Asia* 7(2), 60-69.

Saka, C. (2012). "BET, TG-DTG, FT-IR, SEM, iodine number analyses and preparation of activated carbon from acorn shell by chemical activation with $ZnCl_2$," *J. Anal. Appl. Pyrol*. 95, 21-24. DOI: 10.1016/j.jaap.2011.12.020

Site, A. D. (2001). "Factors affecting sorption of organic compounds in natural sorbent/water systems and sorption coefficients for selected pollutants. A review," *J. Phys. Chem. Ref. Data* 30(1), 187-439. DOI: 10.1063/1.1347984

Sivakumar, V., Asaithambi, M., and Sivakumar, P. (2012). "Physico-chemical and adsorption studies of activated carbon from agricultural wastes," *Adv. Appl. Sci. Res*. 3(1), 219-226

Soleimani, M., and Kaghazchi, T. (2007). "Agricultural waste conversion to activated carbon by chemical activation with phosphoric acid," *Chem. Eng. Technol*. 30(5), 649-654. DOI: 10.1002/ceat.200600325

Subha, R., and Namasivayam, C. (2009). "Zinc chloride activated coir pith carbon as low cost adsorbent for removal of 2,4-dichlorophenol: Equilibrium and kinetic studies," *Ind. J. Chem. Technol*. 16(6), 471-479

Tangjunak, S., Insuk, N., Tontrakoon, J., and Udeye, V. (2009). "Adsorption of Pb(ii) and Cd(II) ions from aqueous solutions by adsorption on activated carbon prepared from cashew nut shells," *Int. Sci. Ind*. 3(4), 1098-1104. DOI: waset.org/Publication/10191

Usman, A. R. A. (2008). "The relative adsorption selectivities of Pb, Cu, Zn, Cd and Ni by soils developed on shale in New Valley, Egypt," *Geoderma* 144(1-2), 334-343. DOI: 10.1016/j.geoderma.2007.12.004

WAC (2012). "World activated carbon," Study #2878, The Freedonia Group, Cleveland, OH.

West, R. C. (1977). "Tidal salt marsh and mangal formations of Middle and South America," in: *Ecosystems of the World. 1. West Coastal Ecosystems*, V. J. Chapman (ed.), Elsevier, Amsterdam, pp. 193-213.

Yeung, P. T., Chung, P. Y., Tsang, H. C., Tang, J. C., Cheng, G. Y., Gambari, R., Chui, C., and Lam, K. H. (2014). "Preparation and characterization of bio-safe activated charcoal derived from coffee waste residue and its application for removal of lead and copper ions," *RSC Adv*. 4(73), 38839-38847. DOI: 10.1039/C4RA05082G

Zaini, M. A. A., Zakaria, M., Alias, N., Zakaria, Z. Y., Johari, A., Setapar, S. H. M., Kamaruddin, M. J., and Yunus, A. C. (2014). "Removal of heavy metals onto KOH-activated ash-rich sludge adsorbent," *Energ. Procedia* 61, 2572-2575. DOI: 10.1016/j.egypro.2014.12.048

Article submitted: June 26, 2015; Peer review completed: September 6, 2015; Revised version received: Sept. 18, 2015; Further revisions and acceptance: November 6, 2015; Published: December 9, 2015.
DOI: 10.15376/biores.11.1.1092-1107